Catalysis Today 155 (2010) 206–213

Contents lists available at ScienceDirect

Catalysis Today

journal homepage: www.elsevier.com/locate/cattod

The observation of equilibria present in stepwise gas phase hydrogenation reactions

Andrew McFarlane [a], Liam McMillan [a], Ian Silverwood [a], Neil G. Hamilton [a], David Siegel [a], Stewart F. Parker [b], David T. Lundie [c], David Lennon [a,*]

[a] Department of Chemistry, Joseph Black Building, University of Glasgow, Glasgow, G12 8QQ, UK
[b] ISIS Facility, Rutherford Appleton Laboratory, Chilton, Didcot, Oxon OX11 0QX, UK
[c] Hiden Analytical Ltd., 420 Europa Boulevard, Warrington, WA5 7UN, UK

ARTICLE INFO

Article history:
Available online 31 December 2009

Keywords:
Pentene hydrogenation
Pentadiene hydrogenation
Infrared spectroscopy
Palladium/alumina catalyst

ABSTRACT

The hydrogenation of a number of C_5 olefins (pent-1-ene, *trans*-pent-2-ene, *cis*-pent-2-ene, *trans*-1,3-pentadiene and a technical mixture of 1,3-pentadiene) over a 1% Pd/Al_2O_3 catalyst has been studied using *in situ* infrared spectroscopic methods to observe the changes in the gas phase molecules during the course of the reaction. Whereas *trans*-pent-2-ene is directly hydrogenated to pentane, the reaction profile for *cis*-pent-2-ene indicates a consecutive process involving the formation of gaseous *trans*-pent-2-ene as a reaction intermediate. Extending these studies to *trans*-1,3-pentadiene shows the terminal double bond to be hydrogenated first to produce *trans*-pent-2-ene in the gas phase, which is then subsequently hydrogenated to the alkane. A reaction scheme is proposed that defines how the molecules are partitioned between the gaseous and adsorbed phases. This scheme makes use of a previously postulated two-site adsorption model. Analysis of a technical grade of 1,3-pentadiene indicates the *trans*-monoene to play a significant role in the stepwise hydrogenation process.

1. Introduction

Within heterogeneous catalysis the application of infrared spectroscopy to probe reactions at the gas–solid interface has a rich heritage [1]. A major thrust in that area has been to operate experiments that emphasize the composition and structure of species present at the catalyst surface [2]. This information is vital in elucidating reaction mechanisms, which can then be used to help design catalysts exhibiting superior catalytic performance in terms of yield and lifetime. However, a variation of the technique that tends to be less widely exploited is to use the infrared spectrum of the reacting gases present over a supported metal catalyst to define the composition of the reacting medium at any one time [3]. Traditionally the preferred analytical approach of monitoring such reactions is generally undertaken using chromatographic techniques (*e.g.* gas–liquid chromatography) or mass spectrometry. However, the *in situ* infrared technique offers the advantage that, providing the reacting components can be satisfactorily identified within a mixture of gases, then the spectrum provides information on gases that are in direct exchange with the catalyst surface. Moreover, it provides information on equilibria that describe how a particular reagent/product is partitioned between the adsorbed and gaseous phases at any one time. Repeated scanning during the course of a reaction sequence then enables reaction profiles to be obtained. Given that all the observed components are in the gaseous phase, where their vibrational intensity is not complicated by adsorption related effects such as dipole coupling [4], then calibration of the associated infrared bands can be readily accomplished as the infrared intensities conform to the Beer–Lambert law [5]. Whilst it is acknowledged that the *in situ* infrared analysis of heterogeneously catalysed gas phase reactions has several limitations (*e.g.* spectral overlap can compromise quantification of particular gases, thereby preventing determination of a mass balance), it does allow identification of thermodynamically accessible reaction pathways. Furthermore, the molecular speciation possible within infrared spectroscopy enables particular stereoisomers to be identified, so the possibility of isomerisation reactions can also be evaluated for a given reaction sequence.

This work concentrates on gas phase hydrogenation reactions, with the hydrogenation of a number of unsaturated C_5 compounds over a supported palladium catalyst selected for investigation. In the first instance this will concentrate on monoenes (1-pentene, *cis*-pent-2-ene and *trans*-pent-2-ene), which will then be extended to dienes (*trans*-1,3-pentadiene and a technical grade of 1,3-pentadiene). The hydrogenation of C_5

* Corresponding author. Tel.: +44 0 141 330 4372; fax: +44 0 141 330 4888.
E-mail address: d.lennon@chem.gla.ac.uk (D. Lennon).

0920-5861/$ – see front matter © 2009 Elsevier B.V. All rights reserved.
doi:10.1016/j.cattod.2009.11.007

molecules is industrially relevant, being closely linked to oil refinery capacity [6].

Regarding previous studies on C_5 olefins, Doyle et al. [7] have examined how Pd nanoparticles compare to Pd single crystals in terms of adsorption characteristics and also reactivity. Canning et al. [8] have examined competitive effects active in the hydrogenation of 1-pentene, *cis*-pent-2-ene and *trans*-pent-2-ene over a commercial grade alumina-supported Pd catalyst. In a related study, Mantle et al. [9] have used polarisation enhanced ^{13}C NMR spectroscopy to examine pentene hydrogenation over a similar commercial Pd/Al_2O_3 catalyst. That work identifies trends in the hydrogenation characteristics of 1-pentene, *cis*-pent-2-ene and *trans*-pent-2-ene but also, importantly, establishes a significant role for *trans*-pent-2-ene in the adsorption/hydrogenation process. In the absence of hydrogen, single component pentene isomers rapidly isomerise to predominantly *trans*-2-pentene. The alumina support is also seen to influence the surface chemistry [9].

1,3-Pentadiene hydrogenation has been comprehensively studied by Wells and Wilson over a series of metal based catalysts [10], with that work demonstrating the importance of the conformational characteristics of the adsorbed diene on the product distribution. These matters are endorsed by Jackson and Monaghan, who examined alkadiene hydrogenation reactions over a commercial Pd/Al_2O_3 catalyst [11].

The work presented here follows on from a previous study by Opara et al. [12] that used infrared spectroscopy to follow the hydrogenation of a technical mixture of 1,3-pentadiene over an alumina-supported palladium catalyst. That work identified the inter-conversion of *cis*-pent-2-ene → *trans*-pent-2-ene as an important part of the reaction sequence. Moreover, via a series of co-adsorption experiments, a two-site model was proposed to explain the kinetic trends observed; with specific sites being responsible for the hydrogenation of the terminal double bond (Site α) and the internal double bond (Site β) of the diene [12].

The Opara study utilised a Pd/Al_2O_3 catalyst derived from palladium chloride [12]. Previous studies from this group have shown residues remaining from the catalyst preparation process can perturb chemisorption properties of the actual working catalyst [13]. In order to check the generality of trends established over the palladium chloride derived catalyst, it was deemed productive to extend those studies to examine reactions over a Pd/Al_2O_3 catalyst that utilises palladium nitrate as the precursor compound. Furthermore, in order to evaluate the relevance of the *trans*-pent-2-ene stereoisomer in the stepwise hydrogenation process of 1,3-pentadiene, the infrared technique was extended to examine a series of monoenes over this catalyst as well. Moreover, the previous study [12] highlighted the paucity of comprehensive vibrational studies of C_5 molecules. Studies of pentane [14] and *cis*- and *trans*-pentadiene [15] are available, as well as a study of 1-pentene on NaX zeolite [16]. Surprisingly, there appears to be few studies on the 2-pentenes. In order to make maximum use of the infrared reactor technique, it is necessary to be able to identify all of the bands of the reagents/products as well as possible intermediate compounds. For example, in the Opara study a feature detected at 940 cm^{-1} when 1,3-pentadiene was hydrogenated over the Pd/Al_2O_3 catalyst could not be readily assigned to any fundamental mode of the candidate molecules. Instead, a combination of inelastic neutron scattering (INS) measurements and computer calculations were used to assign the feature to an out-of-phase C_1–C_2 and C_4–C_5 stretch of *cis*-pent-2-ene [12]. This study adopts a similar multi-technique approach, where INS measurements and computer simulations are used to ensure that any bands that feature in the infrared spectra of the various reaction systems can be comprehensively assigned. In this way, any possible intermediate species should be readily identified within the experimental protocol adopted herein.

2. Experimental

2.1. Catalyst preparation and characterisation

The catalyst containing 1% palladium (w/w) was prepared by impregnation of γ-alumina (BASF Q332, BET surface area 186 $m^2\,g^{-1}$) with palladium nitrate (Sigma–Aldrich, 98%). The desired amount of precursor was dissolved in the minimum amount of water and added drop-wise to a slurry of alumina in water and stirred for 24 h. The solvent was subsequently removed by rotary evaporation and the mixture dried in air at 473 K for 1 h prior to being sieved into particles in the range 250–500 μm. The metal loading of the catalyst was determined to be 1.0% by atomic absorption spectroscopy (Perkin Elmer 1100 Atomic Absorption Spectrometer at 247.6 nm with an acetylene flame). BET analysis revealed the catalyst to have a surface area of 196 $m^2\,g^{-1}$, indicating that the impregnation process had not compromised the total surface area of the alumina. Carbon monoxide pulse chemisorption and desorption experiments were obtained via mass spectrometry using a Hiden Analytical CATLAB facility. The CO-adsorption isotherm revealed a saturation coverage of 6.3 μmol CO $g^{-1}_{(cat)}$. Assuming a Pd:CO stoichiometry of 2:1 [13], this corresponds to 7.6×10^{18} surface Pd atoms g^{-1} (cat) and a metal dispersion of 13.4%. Assuming the metal particles to be spheres of equal diameter, the dispersion corresponds to an estimated mean particle size of 8.3 nm [13]. Samples of the catalyst were examined by transmission electron microscopy using a Joel 1200 FX electron microscope operating at 120 kV, where a mean metal particle size of 8.4 nm was observed that exhibited a relatively broad particle size distribution. The temperature programmed desorption profile for the CO saturated catalyst (not shown) is characterised by two distinct features: (i) a sharp band centred at 580 K that exhibits a discrete shoulder at 600 K and (ii) a broader feature with a maximum at 650 K that tails to higher temperature. The 580 K peak is assigned to CO that is bound to Pd crystallites, whereas the 650 K species is attributed to the (partial) decomposition of carboxy-species that are associated with the alumina support [17].

2.2. Apparatus and reaction testing

The apparatus and general procedure are similar to those described elsewhere [12]. Briefly, the apparatus comprises a modified Graseby-Specac 5660 heated gas cell that is connected to a gas manifold which utilises mass flow devices (Brooks 5850E) to control the flow of hydrogen (BOC, 99.995% purity) and helium (BOC, 99.999% purity) into the cell. The cell is fitted with isolation valves and is housed within a purged Nicolet Avatar 360 FT-IR spectrometer. An injection septum within the cell enables reagents to be added to the reaction system.

The catalyst was loaded into the reactor as a pressed disc. For all the studies presented in this study the catalyst was mounted within a glass sample holder that locates within the base of the cell, so that the catalyst was not in the path of the infrared beam. In this way, all spectra presented arise from the composition of the gaseous phase, with no contribution from the catalyst or the catalyst surface. This simplifies the analysis considerably. The rate of pentadiene and pentene hydrogenation reactions were directly proportional to the mass of catalyst used, indicating the reaction to be under kinetic control with no mass transport restrictions. The catalyst mass, quantity of hydrocarbon and pressure of hydrogen were selected to yield a full hydrogenation profile in a time that was sufficiently long (*ca.* 30 min) so that infrared spectra of sufficient signal/noise ratio could be repeatedly recorded during that interval, in order to define a representative reaction profile. In this manner, 1 part of the 1% Pd/Al_2O_3 catalyst was diluted with 20

parts of the support material (γ-alumina), ground in a pestle and mortar, then *ca.* 100 mg of this mixture was pressed into a thin disc using a 13 mm die (Specac) pressurised at 12 tonnes by a hydraulic press (PerkinElmer). The catalyst disc was reduced in the following manner: the cell temperature was maintained at 303 K and a mixture of 10% H_2/90% He was passed through the reactor at a flow rate of 20 ml min^{-1} for 30 min, then the hydrogen composition was increased to yield an equimolar mixture of hydrogen and helium at the same flow rate. After 5 min the reactor was isolated at a pressure of 900 Torr (0.12 MPa). A liquid chromatography syringe (Hamilton Bonaduz) was used to inject a 10.0 μl aliquot of hydrocarbon reagent into the cell via the septum. Pent-1-ene (Fluke, 95%), *trans*-pent-2-ene (Fluka, 99%), *cis*-pent-2-ene (Aldrich, 98%), *trans*-1,3-pentadiene (Aldrich, 99%) and a technical mixture of 1,3-pentadiene (Aldrich, *ca.* 60% *trans*-1,3-pentadiene/30% *cis*-1,3-pentadiene) were used without further purification. Scanning of the infrared spectrum commenced as soon as the injection of the hydrocarbon was complete. This combination of reagents results in a hydrogen:hydrocarbon ratio of 29:1 and a hydrocarbon:Pd(s) ratio of 1520:1, *i.e.* hydrogen is in excess of the hydrocarbon and the hydrocarbon is in excess of palladium surface atoms. Thus, the infrared cell is acting as a batch reactor under conditions where reasonable conversions represent multiple turnovers, unhindered by the availability of hydrogen. Infrared spectra were recorded at a resolution of 4 cm^{-1}, co-adding eight scans and requiring an acquisition time of *ca.* 10 s. The reaction temperature was maintained at 303 K for all the reactions studied and ensured that all the reagents remained in the gaseous phase. All measurements were performed at least in duplicate, with representative datasets being presented here. Given the relative simplicity of the experimental arrangement, the reacting gases obey the Beer–Lambert law, thereby permitting calibration curves to be readily produced. In this way, the number of moles of the majority of reagents could be reliably determined from the integrated infrared intensity for a particular vibrational feature.

2.3. Inelastic neutron scattering

Inelastic neutron scattering (INS) experiments were performed using the TOSCA spectrometer at the ISIS pulsed spallation neutron facility at the Rutherford Appleton Laboratory. The spectrometer is described in detail elsewhere [18]. Briefly, the spectrometer is an indirect geometry, time of flight spectrometer with a spectral range of 16–4000 cm^{-1}. The resolution of the spectrometer is 1.25% of the energy transfer and frequency precision is ±3 cm^{-1} up to 2000 cm^{-1}. Samples of a number of C_5 molecules (pent-1-ene, *trans*-pent-2-ene, *cis*-pent-2-ene, *trans*-1,3-pentadiene, 1,3-pentadiene (technical mixture), 1,4-pentadiene (Aldrich, 99%), cyclopentane and cyclopentene) were loaded into aluminium liquid cells and transferred on to a carousel that facilitated sequential sampling. The sample holder was connected to a closed cycle refrigerator and cooled to *ca.* 20 K. All INS spectra were recorded at this temperature.

2.4. Computational studies

Density functional theory (DFT) calculations for a series of C_5 molecules (pent-1-ene, *trans*-pent-2-ene, *cis*-pent-2-ene, *trans*-1,3-pentadiene, 1,4-pentadiene, cyclopentane, cyclopentene and pentane) were performed using the B3LYP functional with the 6-311*g(d,p) basis set as implemented in Gaussian-03 [19]. Comparison with the literature values for the main infrared bands of these molecules [20] gave generally good agreement. The GaussView 3.0 package was used for visualisation and subsequent assignment of the vibrational modes. The programme Aclimax [21] used the atomic displacements derived from the Gaussian-03 output to generate the INS spectrum of the C_5 molecules under examination. The calculated and the observed INS spectra compared well, confirming the validity of the calculations and the associated vibrational assignments.

3. Results and discussion

3.1. Vibrational assignments

Vibrational assignments for pent-1-ene, *trans*-pent-2-ene, *cis*-pent-2-ene, *trans*-1,3-pentadiene, 1,4-pentadiene, cyclopentane, cyclopentene and pentane were obtained from analysis of the DFT calculations, which were validated by comparison with INS spectra. As an example of a representative case, Fig. 1 shows (a) the measured and (b) calculated INS spectrum for *cis*-pent-2-ene. Agreement between experiment and theory is good. This outcome validates the calculations, from which the vibrational assignments are derived. Being able to comprehensively justify assignments for reagents, products and possible intermediates, *e.g.* various pentenes via associated wags [12], are important in ensuring reliable identification of reactants present in the gaseous phase during the course of the hydrogenation process. Table 1 lists specific vibrational modes that were used to identify the various reagents. Periodic monitoring of the IR spectrum as a function of time can then be used to determine reaction profiles for specific hydrogenation reactions.

3.2. Blank experiments

Prior to commencing catalysed hydrogenation studies, a series of blank experiments were performed. This involved recording the infrared spectrum as a function of time with a particular hydrocarbon in the reaction cell (*e.g.* 1,3-pentadiene) in the presence of hydrogen and helium but in the absence of the Pd/Al_2O_3 catalyst. No change in the spectra was seen over a 30 min acquisition period. Hydrogenation experiments on an alumina disc showed no conversion of 1,3-pentadiene. These results confirmed the cell to be gas tight and that no hydrogenation reaction takes place under these conditions when no Pd/Al_2O_3 catalyst is present.

3.3. Monoene hydrogenation

3.3.1. Pent-1-ene

Hydrogenation reactions were initiated as outlined in Section 2.2. Integration of particular bands from the infrared spectrum of the gaseous phase as a function of time could then be used to

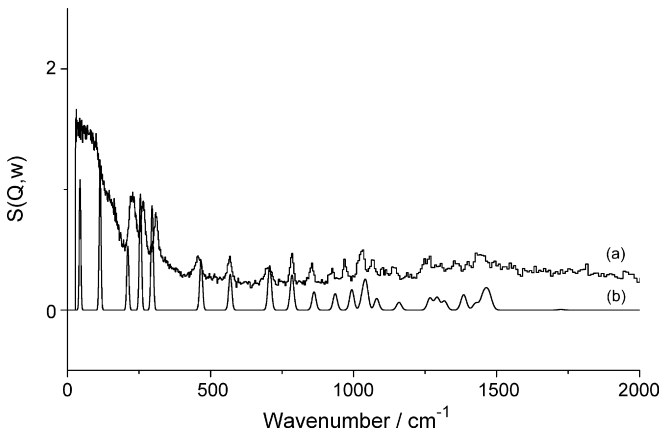

Fig. 1. (a) Measured and (b) simulated inelastic neutron scattering spectrum for *cis*-pent-2-ene. The experimental spectrum was obtained using the TOSCA spectrometer at ISIS, whereas the simulated spectrum required use of the Gaussian-03 and Aclimax computer software.

Table 1
Infrared bands indicative of the range of C_5 molecules under investigation.

Compound	Band position (cm^{-1})	Assignment
Trans-1,3-pentadiene	899 (s)	$=CH_2$ wag
Cis-1,3-pentadiene	621 (s)	*Cis*-CH=CH wag
Cis-1,3-pentadiene	905 (s)	$=CH_2$ wag
Trans-pent-2-ene	969 (s)	In-phase *trans*-CH=CH wag
Cis-pent-2-ene	688 (m)	In-phase *cis*-CH=CH wag
1-Pentene	3087 (s)	Antisymmetric $=CH_2$ C–H stretch
Pentane	2965 (vs)	In-phase antisymmetric CH_3 C–H stretch

obtain a reaction profile for the metal catalysed hydrogenation reactions. Spectral overlap complicated quantification of the pentane contribution in the gaseous mixtures, so it is presented as a peak intensity rather than a molar contribution. Fig. 2 shows the reaction profile for the hydrogenation of pent-1-ene over the Pd/Al_2O_3 catalyst and reveals a simple inter-conversion to pentane, with no other reagents indicated in the spectra. Complete conversion is observed within 25 min.

3.3.2. Trans-pent-2-ene

Fig. 3(a) presents infrared spectrum in the region 800–1100 cm^{-1} for the hydrogenation of *trans*-pent-2-ene, where a single band at 960 cm^{-1} is seen to progressively collapse over a period of 35 min. This feature is assigned to the *trans*-CH=CH wag, that is indicative of the internal double bond. Fig. 3(b) presents the associated reaction profile, which shows a direct transformation from *trans*-pent-2-ene to pentane. The reaction is complete within approximately 40 min, indicating the internal double bond to be less labile to hydrogenation than the terminal double bond.

3.3.3. Cis-pent-2-ene

The infrared spectrum for the hydrogenation of *cis*-pent-2-ene is shown in Fig. 4(a), where bands at 692 and 933 cm^{-1} are seen. The former corresponds to the in-phase *cis*-CH=CH wag of *cis*-pent-2-ene [20], whilst the latter is the out-of-phase C_1–C_2 and C_4–C_5 stretch of *cis*-pent-2-ene [12]. The 692 cm^{-1} band monotonically decreases with time, whereas the 933 cm^{-1} peak shifts to higher wavenumber (958 cm^{-1}), which then decreases in intensity. The 958 cm^{-1} feature is assigned to the *trans*-CH=CH wag of *trans*-pent-2-ene [12]. The presence of this feature is evidence that the *cis*-olefin has been converted to the *trans* stereoisomer. This process is occurring over a timescale that is comparable to the rate of hydrogenation. Continued scanning of the infrared spectrum leads to the presence of a weak feature at 916 cm^{-1}, which is associated with the formation of pentane. A sharp band is present in Fig. 4(a) at a roughly equal intensity in all spectra at 668 cm^{-1}. This is the ν_2 bending mode of carbon dioxide and indicates the presence of a small quantity of air within the optical path of the infrared beam. Most likely this is occurring about the rubber sleeves that connect the sealed gas cell to the spectrometer purge system. It is a minor external contaminant within the optical pathway that plays no part in the chemical transformations under consideration here.

The reaction profile is presented in Fig. 4(b), the shape of which is consistent with a consecutive process. Specifically, it is suggested that *cis*-pent-2-ene is isomerised to *trans*-pent-2-ene,

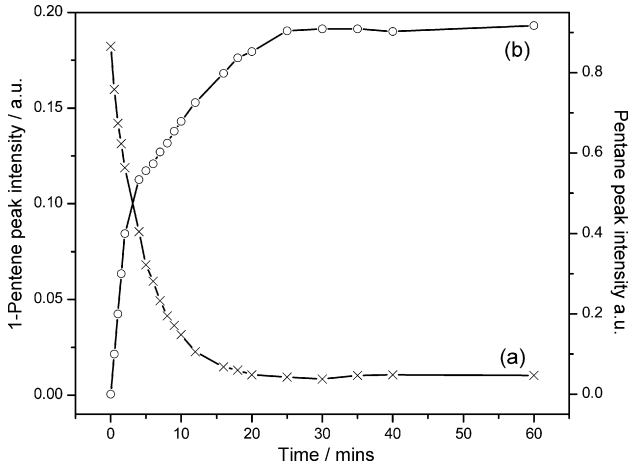

Fig. 2. Reaction profile for the hydrogenation of 1-pentene over 1% Pd/Al_2O_3: (a) 1-pentene and (b) pentane. The antisymmetric $=CH_2$ C–H stretch at 3087 cm^{-1} and the in-phase antisymmetric CH_3 C–H stretch at 2965 cm^{-1} have respectively been used to quantify 1-pentene and pentane contributions.

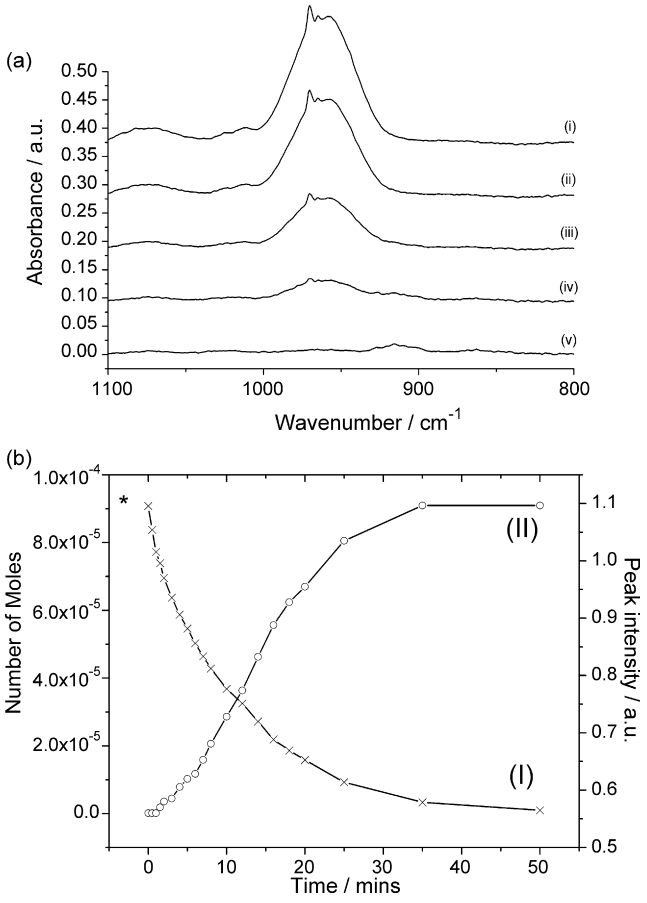

Fig. 3. (a) The infrared spectrum (800–1100 cm^{-1}) corresponding to the hydrogenation of *trans*-pent-2-ene over 1% Pd/Al_2O_3 as a function of time. Spectra were acquired at the following times following injection of the hydrocarbon: (i) 0 min, (ii) 2 min, (iii) 10 min, (iv) 20 min and (v) 35 min. (b) Reaction profile for the hydrogenation of *trans*-pent-2-ene over 1% Pd/Al_2O_3: (I) *trans*-pent-2-ene and (II) pentane. The in-phase *trans*-CH=CH wag at 969 cm^{-1} and the in-phase antisymmetric CH_3 C–H stretch at 2965 cm^{-1} have respectively been used to quantify *trans*-pent-2-ene and pentane contributions. The asterisk (*) represents the initial concentration of *trans*-pent-2-ene.

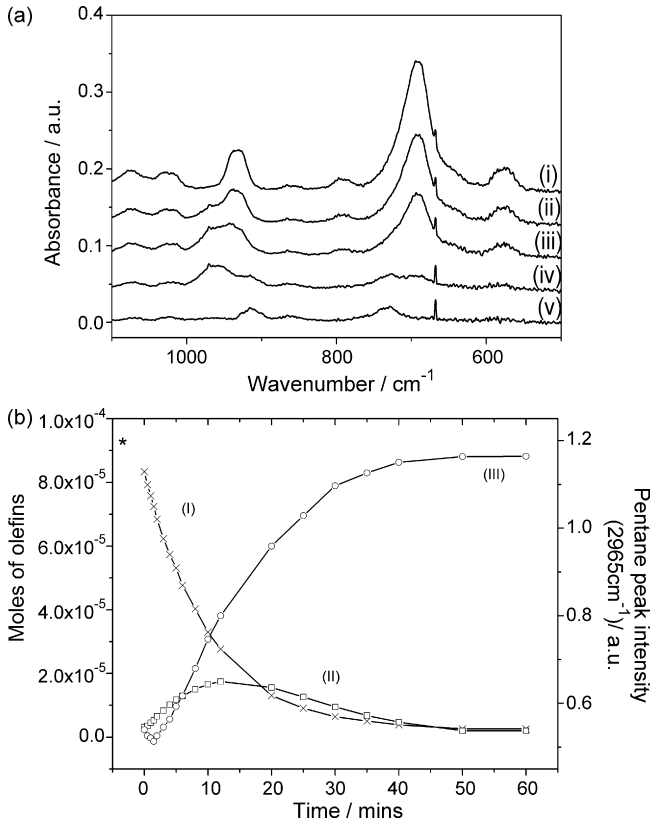

Fig. 4. (a) The infrared spectrum (500–1100 cm^{-1}) corresponding to the hydrogenation of *cis*-pent-2-ene over 1% Pd/Al_2O_3 as a function of time. Spectra were acquired at the following times following injection of the hydrocarbon: (i) 0 min, (ii) 15 min, (iii) 30 min, (iv) 45 min and (v) 60 min. (b) Reaction profile for the hydrogenation of *cis*-pent-2-ene over 1% Pd/Al_2O_3: (I) *cis*-pent-2-ene, (II) *trans*-pent-2-ene and (III) pentane. The in-phase *cis*-CH=CH wag at 688 cm^{-1}, the in-phase *trans*-CH=CH wag at 969 cm^{-1} and the in-phase antisymmetric CH_3 C–H stretch at 2965 cm^{-1} have respectively been used to quantify *cis*-pent-2-ene, *trans*-pent-2-ene and pentane contributions. The asterisk (*) represents the initial concentration of *cis*-pent-2-ene.

which is then selectively hydrogenated to produce the saturated alkane (pentane). A reaction scheme indicating how the reagents are partitioned between the gaseous and chemisorbed phases is presented in Fig. 5, which comprises a series of sequential equilibria. A benefit of this *in situ* infrared spectroscopic approach is that the spectrum provides evidence for the equilibrium reactions present over the catalyst surface, with repeated scanning additionally providing kinetic information. For example, Fig. 4(b) shows the hydrogenation to be complete within about 40 min, which is consistent with that seen earlier for hydrogenation of the internal double bond (Section 3.3.2).

Collectively, Figs. 3 and 4 indicate that, for this catalyst, hydrogenation of the internal bond occurs via *trans*-pent-2-ene and, should the catalyst be presented with *cis*-pent-2-ene, it will first isomerise the reagent to the *trans* form prior to the hydrogenation step. It is acknowledged however that the experimental approach adopted here precludes detection of any *cis*-pent-2-ene that could be retained on the catalyst surface. Hence Fig. 5 only attempts to describe pathways discernible via the existing procedures. The overlap of bands primarily associated with pentane mitigates against determination of a mass balance, which further constrains the analysis. Nevertheless, the realisation of the observed *cis*-pent-2-ene/*trans*-pent-2-ene isomerisation process has important implications in understanding the hydrogenation characteristics of the C_5 molecules under investigation.

3.4. Pentadiene hydrogenation

3.4.1. Trans-1,3-pentadiene

The reaction profile for *trans*-1,3-pentadiene hydrogenation is shown in Fig. 6. Consumption of the starting material is rapid (full conversion *ca.* 20 min) and coincides with the presence of

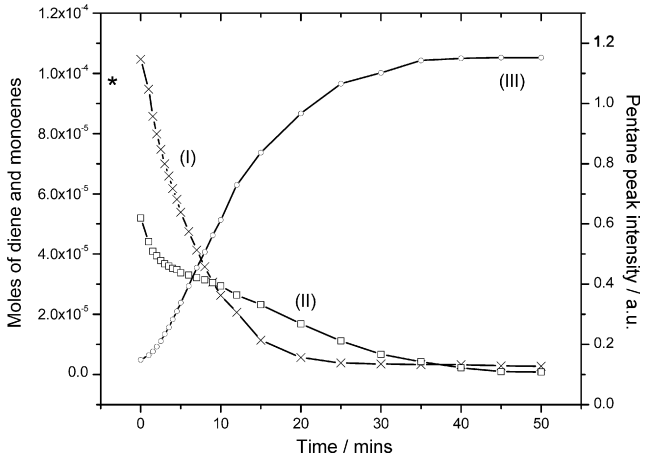

Fig. 6. Reaction profile for the hydrogenation of *trans*-1,3-pentadiene over 1% Pd/Al_2O_3: (I) *trans*-1,3-pentadiene, (II) *trans*-2-pentene and (III) pentane. The $=CH_2$ wag at 899 cm^{-1}, the in-phase *trans*-CH=CH wag at 969 cm^{-1} and the in-phase antisymmetric CH_3 C–H stretch at 2965 cm^{-1} have respectively been used to quantify *trans*-1,3-pentadiene, *trans*-pent-2-ene and pentane contributions. The asterisk (*) represents the initial concentration of *trans*-1,3-pentadiene.

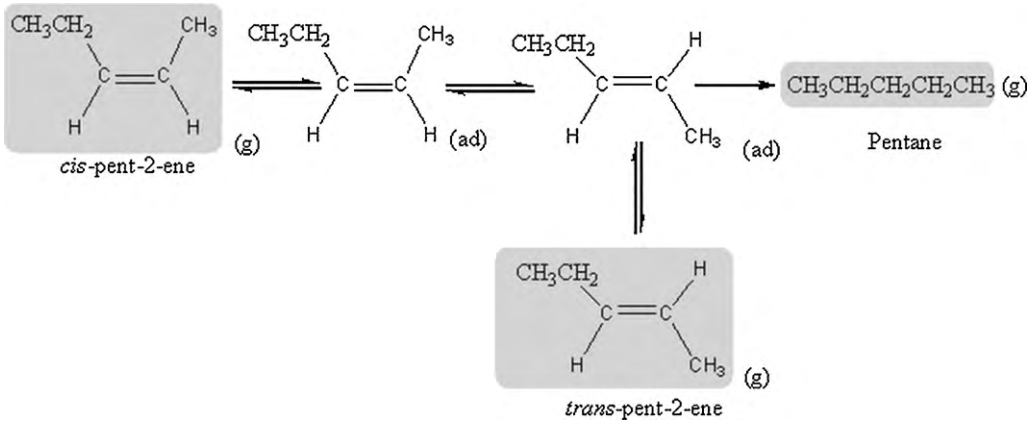

Fig. 5. Reaction scheme for the hydrogenation of *cis*-pent-2-ene over 1% Pd/Al_2O_3. Subscripts (g) and (ad) respectively correspond to gaseous and adsorbed phases. The shaded boxes relate to the gas phase species identifiable in the infrared measurements.

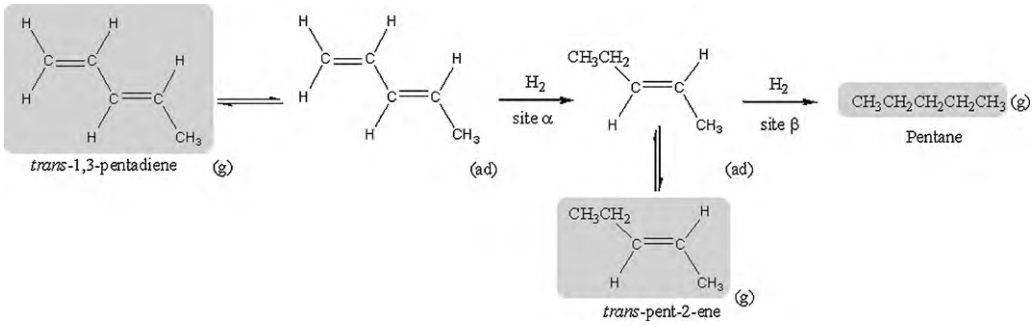

Fig. 7. Reaction scheme for the hydrogenation of *trans*-1,3-pentadiene over 1% Pd/Al_2O_3. Subscripts (g) and (ad) respectively correspond to gaseous and adsorbed phases. The shaded boxes relate to the gas phase species identifiable in the infrared measurements. Sites α and β are described within the text (Section 3.4.1) and respectively relate to hydrogenation of the terminal and internal double bonds.

trans-pent-2-ene in the gaseous phase, which is then hydrogenated to form pentane. Crucially, no *cis*-pent-2-ene or pent-1-ene is detected at any stage of the reaction sequence indicating the absence of isomerisation steps in this instance. Fig. 6 can be readily interpreted as representing a consecutive process where the internal double bond of the *trans*-1,3-pentadiene is hydrogenated first to form *trans*-pent-2-ene. It is noted that the duration of the first stage hydrogenation is comparable to that seen for the terminal double bond (Fig. 2, pent-1-ene, reaction complete within *ca.* 20 min), whilst the second stage hydrogenation is comparable to that seen for the internal double bond (Figs. 3 and 4, pent-2-ene, reaction complete within *ca.* 40 min).

Fig. 7 indicates how the reagents are partitioned between adsorbed states and the gas phase. The fact that the time taken for hydrogenation of the terminal and internal double bonds for the diene compares favourably for the time taken for the hydrogenation of the respective monoenes (Section 3.3) is suggestive that first and second stage hydrogenation is taking place at different sites that are operating independently of one another. Such an arrangement is consistent with the profile presented in Fig. 6 and indicates a two-site model to be valid in this case. Previous work on examining hydrogenation of 1,3-pentadiene over a $PdCl_2$-derived alumina-supported catalyst also invoked a two-site model [12]. There, kinetic comparisons between hydrogenation rates for terminal and internal double bonds were backed up by co-adsorption studies that demonstrated how a modifier (toluene-d_8) selectively perturbed specific sites. Site α was assigned to Pd sites that exclusively hydrogenated the terminal double bond, whilst hydrogenation of the internal double bond took place at Site β. Moreover, isomerisation reactions were tentatively ascribed to occur at Site α [12]. Comparing the reaction characteristics presented in Figs. 2–6, it appears that a two-site model is equally applicable to the hydrogenation activity of the $Pd(NO_3)_2$-derived catalyst examined here, thereby permitting the original site labels (α and β) to be similarly applied. In this manner, the roles for these sites are specified within Fig. 7.

As this work has not included modifier studies, it is not possible to be specific regards the origin of the site responsible for isomerisation processes on this catalyst. This matter is not directly applicable to *trans*-1,3-pentadiene hydrogenation and therefore does not feature in Fig. 7. However, it does connect with aspects of the surface chemistry seen in the hydrogenation of *cis*-pent-2-ene (Section 3.3.3) and also when *cis*-1,3-pentadiene is present (see Section 3.4.2). Whereas it is tempting to extrapolate from the studies on the $PdCl_2$-derived catalyst and to associate Site α with this role [12], it is acknowledged that further work is necessary to establish any similar connection for this catalyst. Consequently, the application of the two-site model will be constrained here to just consider hydrogenation steps and will not be extended to the important issue of isomerisation processes.

3.4.2. Technical grade 1,3-pentadiene

The reaction profile for the technical grade of 1,3-pentadiene (*ca.* 60% *trans*/30% *cis*) is shown in Fig. 8, which is seen to be more involved than the preceding cases. With reference to Table 1, the $=CH_2$ wag at 900 cm^{-1} is diagnostic for 1,3-pentadiene, as this single band is comprised of contributions from both *trans*-1,3-pentadiene at 899 cm^{-1} and *cis*-1,3-pentadiene at 905 cm^{-1}. However, at the 4 cm^{-1} resolution element utilised in these studies, these features are indistinguishable, enabling the calibrated band intensity of this feature to determine the amount of 1,3-pentadiene (*i.e. cis-* + *trans-*) present throughout the course of the full reaction sequence.

The pentadiene consumption coincides with pentane formation, with both *trans*-pent-2-ene and *cis*-pent-2-ene detected as intermediates that spend time in the gaseous phase above the catalyst. No other reagents are detected. The concentration of *trans*-pent-2-ene significantly exceeds the *cis* isomer, with the former concentration progressively falling over the 60 min duration studied. In contrast the low concentration of *cis*-pent-2-ene exhibits a shallow maximum at about 15 min before progressively reducing to zero at 50 min. Fig. 8 certainly indicates a significant role for the *trans*-monoene and, although somewhat ambiguous, it is possible that a similar isomerisation step as seen for *cis*-pent-2-ene (Fig. 4) is active in this case. Fig. 9 presents a proposed reaction scheme, where pentane formation exclusively involves *trans*-pent-2-ene. Extending the concepts of the two-site model beyond that postulated in the *trans*-1,3-pentadiene studies

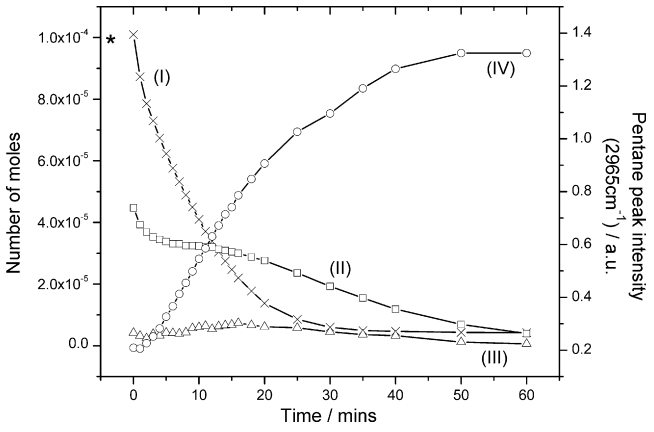

Fig. 8. Reaction profile for the hydrogenation of 1,3-pentadiene (technical mixture) over 1% Pd/Al_2O_3: (I) 1,3-pentadiene, (II) *trans*-pent-2-ene, (III) *cis*-2-pentene and (IV) pentane. The $=CH_2$ wag at 900 cm^{-1}, the in-phase *trans*-CH=CH wag at 969 cm^{-1}, in-phase *cis*-CH=CH wag at 688 cm^{-1} and the in-phase antisymmetric CH_3 C–H stretch at 2965 cm^{-1} have respectively been used to quantify 1,3-pentadiene, *trans*-pent-2-ene, *cis*-pent-2-ene and pentane contributions. The asterisk (*) represents the initial concentration of 1,3-pentadiene.

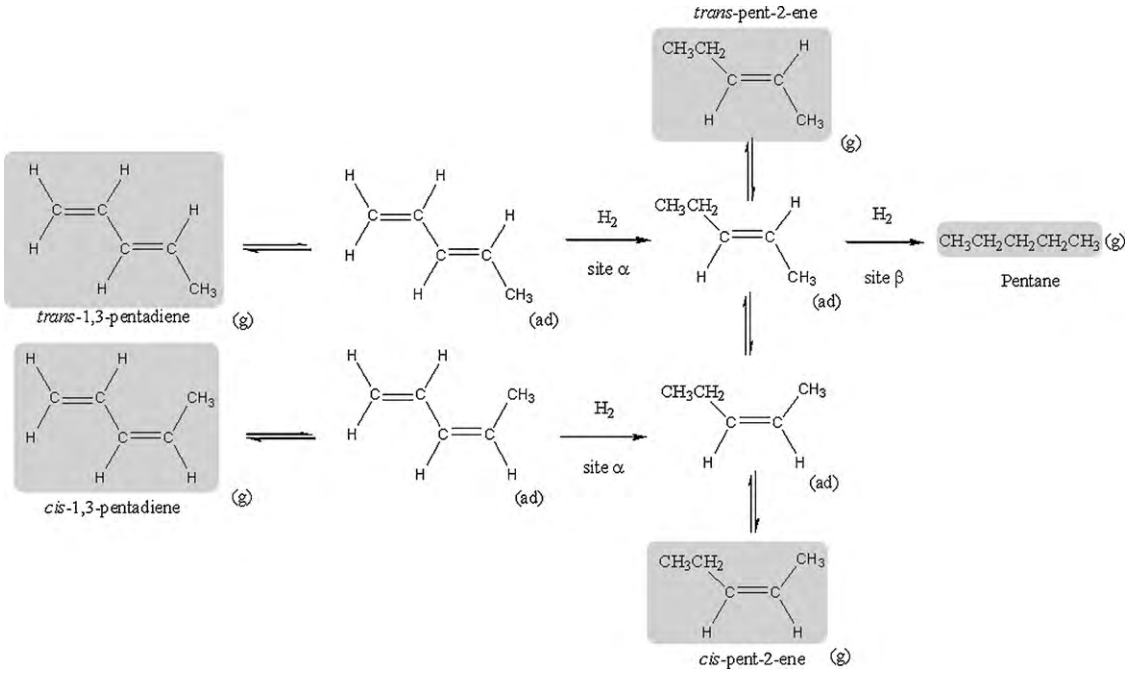

Fig. 9. Proposed reaction scheme for the hydrogenation of a mixture of *trans*- and *cis*-1,3-pentadiene over 1% Pd/Al_2O_3. Subscripts (g) and (ad) respectively correspond to gaseous and adsorbed phases. The shaded boxes relate to the gas phase species identifiable in the infrared measurements. Sites α and β respectively relate to hydrogenation of the terminal and internal double bonds.

(Fig. 7), the reaction scheme again specifies roles for Sites α and β. Further work is necessary to confirm the validity of these proposals. In particular the nature of the site responsible for the isomerisation step needs to be defined but, nevertheless, inspection of Figs. 5–9 shows how the analysis of just the gaseous phase can lead on to suggestions for how a number of equilibria involving reagents partitioning between gaseous and bound phases can contribute to the overall surface chemistry.

4. Summary

The use of an infrared cell as a batch reactor set up to monitor the composition of the gas phase during the course of a number of metal catalysed hydrogenation reactions demonstrates considerable potential in identifying how molecules can partition between gaseous and adsorbed phases. The work presented here has been used to postulate reaction schemes for the hydrogenation of C_5 monoene and diene molecules. These schemes have included (i) an isomerisation step in particular cases and (ii) the proposal that distinct sites on the metal surface are responsible for hydrogenating the internal and terminal double bonds of the olefins. Further work is required to investigate whether the alumina contributes to the observed chemistry. Mantle et al. [9] report that, for their catalyst, the alumina support material was capable of hydrogenating *trans*-pent-2-ene. An investigation on the role of the support material was beyond the scope of the current work.

In the case of the dienes, the internal double bond is seen to hydrogenate first. The batch reactor configuration as opposed to a flow through micro-reactor allows reactions to go towards completion, thereby reflecting the pathways that are thermodynamically favourable under the chosen reaction conditions. Identifying these pathways can then inform practitioners how to set up flow-reactors, which could be used to distort the product distribution in favour of kinetically favoured products.

One of the reasons for commencing this investigation was to discover whether concepts developed for monoene and diene hydrogenation reactions using a $PdCl_2$-derived catalyst [12], that is known to contain chlorine residues [13], could be replicated when using a generic $Pd(NO_3)_2$-derived catalyst. Previous studies using CO chemisorption combined with infrared spectroscopy have demonstrated comparable nitrate-derived catalysts not to be complicated by the presence of chemical residues [13]. On the basis that the reaction trends presented here essentially mimic those observed previously [12], it is concluded that the chlorine residues are not unduly perturbing the C=C hydrogenation chemistry under investigation here. Furthermore, it appears that to a first approximation, both catalysts are providing a similar distribution of sites: designated Sites α and β, which convey similar characteristics on both substrates.

Whilst the attributes outlined above represent strong positives, one additionally needs to acknowledge inherent weaknesses in the method. The use of chemometric procedures is desirable to determine certain band intensities in regions of the spectrum where there is spectral overlap. This issue impedes the determination of reliable mass balances and reveals a clear advantage for the use of conventional chromatographic methods as a primary analytical tool. Finally, it is worthwhile mentioning that the gas phase technique could be nicely complemented by a parallel investigation that concentrates on the adsorbed species. The cell described in this study is equipped with a glass sample holder that permits the pressed disc to be retained below the infrared beam (as was the case in this study) or, alternatively, directly in the path of the infrared beam. A combination of both approaches should provide considerable insight as to the main stages in the related surface chemistry that are responsible for the observed chemical transformations. Not least it should address the issue raised in Section 3.3, namely whether *cis*-pent-2-ene is selectively adsorbed on the catalyst surface and therefore makes minimal contribution to the gas phase infrared spectrum.

5. Conclusions

An investigation was undertaken using infrared spectroscopy to follow the hydrogenation of a number of unsaturated C_5 molecules over a 1% Pd/Al_2O_3 surface at 303 K. The main findings can be summarised as follows:

- Studies on pent-1-ene indicate the terminal double bond to be hydrogenated within *ca*. 20 min.
- Hydrogenation of *trans*- and *cis*-pent-2-ene show the internal double bond to be fully hydrogenated within *ca*. 40 min. Whereas *trans*-pent-2-ene leads directly to pentane, it appears that *cis*-pent-2-ene first isomerises to *trans*-pent-2-ene prior to hydrogenation to pentane. The timescale of the isomerisation step is comparable to that of the hydrogenation step.
- *Trans*-1,3-pentadiene is consumed within *ca*. 20 min, whilst the intermediate *trans*-pent-2-ene is consumed within 40 min. These observations are indicative of the catalyst offering two distinct sites: Site α is responsible for hydrogenation of terminal double bonds and Site β hydrogenates internal double bonds. These sites operate independently.
- Hydrogenation of a technical grade of 1,3-pentadiene (comprising a mixture of *cis*- and *trans*-1,3-pentadiene) suggests a major role for *trans*-pent-2-ene in the hydrogenation process.

Acknowledgements

The EPSRC are thanked for the provision of equipment, a studentship (AMcF) and a Research Fellowship (IS) (Grant EP/E028861/1). Hiden Analytical Ltd. are thanked for technical support and financial assistance. The ISIS Facility, Rutherford Appleton Laboratory is thanked for access to neutron scattering facilities as well as a project studentship (NGH). Syngenta UK Ltd. and the University of Glasgow are thanked for a project studentship (LMcM). The Scottish Higher Education Funding Council assisted with equipment funding via a Research Development Grant.

References

[1] G. Busca, Catal. Today 27 (1996) 323.
[2] V.A. Matyshak, O.V. Krylov, Catal. Today 25 (1995) 1.
[3] S.D. Jackson, S. Munro, P. Colman, D. Lennon, Langmuir 16 (2000) 6519.
[4] P. Hollins, Surf. Sci. Rep. 16 (1992) 51.
[5] B.P. Straughan, S. Walker, Spectroscopy, vol. 2, Chapman and Hall, London, 1976.
[6] K. Weissermel, H.-J. Arpe, Industrial Organic Chemistry, VCH, Weinheim, 1997.
[7] A.M. Doyle, Sh.K. Shaikhutdinov, H.-J. Freund, J. Catal. 223 (2004) 444.
[8] A.S. Canning, S.D. Jackson, A. Monaghan, T. Wright, Catal. Today 116 (2007) 22.
[9] M.D. Mantle, P. Steiner, L.F. Gladden, Catal. Today 114 (2006) 412.
[10] P.B. Wells, G.R. Wilson, J. Chem. Soc. A (1970) 2442.
[11] S.D. Jackson, A. Monaghan, Catal. Today 128 (2007) 47.
[12] E. Opara, D.T. Lundie, T. Lear, I.W. Sutherland, S.F. Parker, D.L. Lennon, Phys. Chem. Chem. Phys. 6 (2004) 5588.
[13] T. Lear, R. Marshall, J.A. Lopez-Sanchez, S.D. Jackson, T.M. Klapötke, M. Bäumer, G. Rupprechter, H.-J. Freund, D. Lennon, J. Chem. Phys. 123 (2005) 174706.
[14] N.G. Mirkin, S. Krimm, J. Phys. Chem. 97 (1993) 13887.
[15] D.A.C. Compton, W.O. George, W.F. Maddams, J. Chem. Soc., Perkin 2 (1977) 1311.
[16] T. Armaroli, E. Finocchio, G. Busca, S. Rossini, Vibrat. Spectrosc. 20 (1999) 85.
[17] T. Lear, N.G. Hamilton, D. Lennon, Catal. Today 126 (2007) 219.
[18] P.C.H. Mitchell, S.F. Parker, A.J. Ramirez-Cuesta, J. Tomkinson, Vibrational Spectroscopy with Neutrons with Applications in Chemistry, Biology, Materials Science and Catalysis, World Scientific, Singapore, 2004.
[19] M.J. Frisch, et al., Gaussian 03W, Version 6. 0, Gaussian, Inc., Pittsburgh, PA, 2003.
[20] D. Lin-Vien, N.R. Colthup, W.G. Fateley, J.G. Grasselli, The Handbook of Infrared and Raman Characteristic Frequencies of Organic Molecules, Academic Press, London, 1991.
[21] A.J. Ramirez-Cuesta, Comp. Phys. Commun. 157 (2004) 226.